VERTICAL IMAGE WAVES IN ELLIPTICALLY ANISOTROPIC MEDIA

J. Schleicher, A. Novais, and J. C. Costa

email: *js@ime.unicamp.br*

keywords: *Image waves, elliptic anisotropy, vertical stretch*

ABSTRACT

By reparameterization of the kinematic expressions for remigration in elliptically anisotropic media using a new ellipticity parameter, we derive a new image wave equation in elliptically anisotropic media describing the position of the reflector as a function of the medium ellipticity. This image wave equation, which is a kind of medium-dependent one-way wave equation, can be used for automatically stretching a time-migrated image in depth until wells are tied or other given geologic criteria are met. In this way, it is possible to find an estimate of the vertical velocity, which cannot be detected from time processing only. A simple numerical example confirms the validity of the theory.

INTRODUCTION

Seismic migration aims at correctly positioning images of seismic reflectors in time or depth sections. For this purpose, a macrovelocity model is needed that is kinematically equivalent to the true velocity distribution in the earth. If the migration velocity model is incorrect, so will be the positioning of the reflector images.

When one of the parameters used for the migration process, generally the velocity model, is altered, the construction of an updated image becomes necessary. This can be achieved either by a new migration of the original data or by a process called "remigration" applied to the previously constructed image. For small changes in the velocity model, remigration has become known as "residual migration" (Rocca and Salvador, 1982; Rothman et al., 1985) or "cascaded migration" (Larner and Beasley, 1987). A continuous change in migration velocity has been termed "velocity continuation" (Fomel, 1994).

In a set of migrated sections obtained using only slightly different velocity model parameters, the reflector images are dislocated only slightly from one to the next. Thus, looking at such a set in fast sequence creates the impression of looking at snapshots of a propagating wavefront. Under the assumption of a constant migration velocity, this "propagation" of reflector images can be described by partial differential equations (Fomel, 1994) that have been termed "image-wave equations" by Hubral et al. (1996).

Since the pioneering work of Fomel (1994), many different image-wave equations for different situations have been proposed and their applications have been studied Jaya (1997); Jaya et al. (1999); Fomel (2003b,a). Although their theory is strictly valid only in homogeneous media, image-wave remigration has been successfully applied in inhomogeneous media (Schleicher et al., 2004; Novais et al., 2005). Recently, Schleicher and Aleixo (2007) have extended the theory of image-wave remigration to in media with elliptical anisotropy, which can be described analytically with one single additional medium parameter (see also Aleixo and Schleicher, 2004; Schleicher and Aleixo, 2005). They chose the parameter describing the medium ellipticity to be the ratio between the squares of the vertical and horizontal velocities. Using this parametrization, they showed that time remigration with image waves in elliptically anisotropic media is achieved with the isotropic image wave equation, where the migration velocity is substituted by the horizontal velocity. In other words, the position of a time-migrated reflector image in an elliptically

inhomogeneous medium is independent of the vertical velocity and depends only on the variation of the horizontal velocity. This observation is in agreement with the findings of Alkhalifah and Tsvankin (1995).

Based on this observation, it is more reasonable to assume that from time processing, a good estimate of the horizontal velocity is known, rather than of the vertical velocity. Therefore, in this paper, we reparameterize the equations for elliptical anisotropy. Using a new ellipticity parameter, being the ratio between vertical and horizontal velocity, we derive a new image wave equation in elliptically anisotropic media. This image wave equation, which is much simpler than the previous one, can be used for depth stretching a time-migrated image until given geologic criteria are met.

Of course, elliptic anisotropy is a rather simplistic approximation to the real world. Nonetheless, it can be considered an ideal link from isotropy to anisotropy. Compared to isotropy, it presents an additional degree of freedom that should be sufficient in many cases to improve well-ties by simple ellipticity propagation of the migrated image, On the other hand, compared to more realistic types of anisotropy, it has the advantage that only one additional parameter needs to be determined from the data.

VERTICAL IMAGE WAVES

Seismic remigration tries to establish a relationship between two media of wave propagation in such a way that identical seismic surveys on their respective surfaces would yield the same seismic data. One of these media is the wrong velocity model used for the original migration. The other medium represents the updated model within which a new image of the subsurface needs to be constructed.

Therefore, the kinematic relationship between these two media is established by equaling the traveltimes of a seismic wave in both of them.

In the parametrization of Schleicher and Aleixo (2005, 2007), the traveltime of a zero-offset event with source and receiver at point $(\xi, \eta, 0)$ on the surface and reflection point at (x, y, z) in depth in an elliptically anisotropic medium is given by

$$T(\xi, \eta; x, y, z) = \frac{2}{v}\sqrt{\varphi\left[(x-\xi)^2 + (y-\eta)^2\right] + z^2}, \tag{1}$$

where the parameter describing the medium ellipticity is

$$\varphi = \frac{v^2}{u^2}. \tag{2}$$

Here, u and v are the horizontal and vertical velocities, respectively.

Actually, this parametrization would be useful if the vertical velocity v was known and the horizontal velocity u was unknown. However, time processing in elliptically inhomogeneous media depends only on the horizontal and not on the vertical velocity (Alkhalifah and Tsvankin, 1995). Therefore, a better parametrization, reflecting this fact, uses the new ellipticity parameter γ, defined as

$$\gamma = \frac{u}{v}. \tag{3}$$

Using this new parametrization, the traveltime (equation 1) can be rewritten as

$$T(\xi, \eta; x, y, z) = \frac{2}{u}\sqrt{(x-\xi)^2 + (y-\eta)^2 + \gamma^2 z^2}. \tag{4}$$

The desired kinematic relationship between two media with different ellipticity γ can now be expressed by equaling the above traveltime (equation 4) to the corresponding one for a reflection point (x_0, y_0, z_0) in a medium with identical horizontal velocity u but different ellipticity γ_0,

$$T(\xi, \eta; x_0, y_0, z_0) = \frac{2}{u}\sqrt{(x_0-\xi)^2 + (y_0-\eta)^2 + \gamma_0^2 z_0^2}. \tag{5}$$

The identity of the two traveltimes (equations 4 and 5) yields the expression

$$F = (x_0-\xi)^2 + (y_0-\eta)^2 + \gamma_0^2 z_0^2 - \left[(x-\xi)^2 + (y-\eta)^2 + \gamma^2 z^2\right] = 0. \tag{6}$$

This expression describes, for each pair (ξ, η), the set of points (x, y, z) that have the same traveltime at the source-receiver position $(\xi, \eta, 0)$ in a medium with ellipticity γ as the point (x_0, y_0, z_0) in the medium with ellipticity γ_0.

Since this identity must be fulfilled independently of the source coordinates, the derivatives of F with respect to ξ and η must be zero, too. From these conditions, we immediately obtain

$$\frac{\partial F}{\partial \xi} = 2(\xi - x_0) - 2(\xi - x) = 0 \tag{7}$$

and

$$\frac{\partial F}{\partial \eta} = 2(\eta - y_0) - 2(\eta - y) = 0. \tag{8}$$

The last two equations can be interpreted as envelope conditions, describing the envelope of the family of curves (equation 6) when varying ξ and η, respectively. These envelopes describe the positions of the so-called Huygens image waves, because their role for image-wave propagation is the same as that of Huygens waves for physical wave propagation. Generally these kind of equations will result in stationary values for ξ and η. Here, they simply provide

$$x = x_0 \tag{9}$$

$$y = y_0. \tag{10}$$

From the above equations, we recognize that the Huygens image waves for this type of image-wave propagations are degenerated to single points moving along the vertical direction. Note that for physical wave propagation in a homogeneous medium, Huygens waves are spheres around the initial point. For isotropic velocity continuation to higher and lower velocities, the Huygens image waves are the lower parts of rotational ellipsoids and hyperboloids, respectively, centered at the surface position $(x_0, y_0, 0)$ above the reflection point (x_0, y_0, z_0).

The actual expression for the Huygens image wave is obtained from substitution of these last two identities back into the expression for F, resulting in

$$\gamma_0^2 z_0^2 = \gamma^2 z^2. \tag{11}$$

Thus, we can establish the simple relationship between the coordinates of the reflection points in the media with ellipticities γ_0 and γ as

$$z = \frac{\gamma_0}{\gamma} z_0. \tag{12}$$

Note that the depth stretching relationship (equation 12) is itself an interesting result. It states how the depth of a reflector changes when the medium ellipticity is changed from γ_0 to γ. Thus, we could reposition the migrated reflector image by picking its depth, calculation the new depth according to the stretch (equation 12) and replace it accordingly. However, for a whole reflector image, this would be a tedious task.

Image-wave equation

For the purpose of deriving an image-wave equation that describes the propagation of the reflector image from one depth to the other for the whole section at once, it is more useful to recast equation 12 into the form

$$\gamma = \gamma_0 \frac{z_0}{z}. \tag{13}$$

In this form, we can interpret this equation as an expression of the type

$$\gamma = \Gamma(x, y, z), \tag{14}$$

with $\Gamma(x, y, z)$ given by

$$\Gamma(x, y, z) = \gamma_0 \frac{z_0}{z}. \tag{15}$$

The function $\Gamma(x, y, z)$ corresponds to an eikonal associated with the image-wave propagation. By taking its derivatives with respect to the coordinates, here due to the simplicity of the eikonal (expression 15) only with respect to z, we can eliminate the initial conditions z_0 and γ_0 from equation 13 to obtain

$$\frac{\partial \Gamma}{\partial z} = -\gamma_0 \frac{z_0}{z^2} = -\frac{\Gamma}{z}. \tag{16}$$

Since Γ is the eikonal of the image-wave propagation, this last identity can be understood as the corresponding eikonal equation.

Note that in deriving the eikonal equation (expression 16) from the eikonal (expression 15), we are inverting the standard flux of derivation. The reason is we want to describe the propagation of the reflector image by a partial differential equation that is valid for any arbitrary initial conditions, while our above considerations were carried out for a single reflection point.

In the same spirit of inverted derivation, we conclude now that any partial differential equation of the type

$$p_z = \frac{\gamma}{z} p_\gamma + \mathcal{F}(x, y, z, p) \tag{17}$$

leads, upon the substitution of a high-frequency (ray-type) ansatz $p = p_0 f[\gamma - \Gamma(x, y, z)]$, in first-order approximation to exactly the above eikonal equation. Thus, all partial differential equations of this type, particularly the one with $\mathcal{F} = 0$, correctly describe the kinematics of the image-wave propagation. Since we are, at this time, not interested in attaching a physical meaning to the amplitudes of image-wave propagation, we can thus choose the simplest of these equations. Therefore, the image-wave equation for propagation in the ellipticity parameter γ is

$$p_z = \frac{\gamma}{z} p_\gamma. \tag{18}$$

As shown in the Appendix, this equation remains valid for depth continuation of a migrated image obtained from offset data.

It is important to observe that the derived image-wave equation does not depend on the lateral coordinates of the reflection point, nor on the actual values of the horizontal and vertical velocities. For this reason, this equation is very promising even for inhomogeneous media.

FD IMPLEMENTATION

The image-wave equation for propagation of a seismic reflector image in γ (equation 18) is a partial differential equation of a very simple type. In fact, it is a kind of advection equation or one-dimensional one-way wave equation with variable propagation velocity $c = z/\gamma$. The numerical solution of the advection equation is probably the best-studied problem in the numerical analysis of partial differential equations. A second-order finite-difference solution is obtained from approximating the γ derivative with a difference centered at an intermediate grid point $j + 1/2$, i.e.,

$$\left.\frac{\partial p}{\partial \gamma}\right|_k^{j+1/2} \approx \frac{p(z_k, \gamma_{j+1}) - p(z_k, \gamma_j)}{\gamma_{j+1} - \gamma_j} = \frac{p_k^{j+1} - p_k^j}{\Delta\gamma}, \tag{19}$$

and the z derivative at the same intermediate point as the mean value between the two centered derivatives at j and $j + 1$, i.e.,

$$\left.\frac{\partial p}{\partial z}\right|_k^{j+1/2} \approx \frac{1}{2}\left(\frac{p(z_{k+1}, \gamma_j) - p(z_{k-1}, \gamma_j)}{z_{k+1} - z_{k-1}} + \frac{p(z_{k+1}, \gamma_{j+1}) - p(z_{k-1}, \gamma_{j+1})}{z_{k+1} - z_{k-1}}\right) \tag{20}$$

$$\approx \frac{1}{4}\left(\frac{p_{k+1}^j - p_{k-1}^j}{\Delta z} + \frac{p_{k+1}^{j+1} - p_{k-1}^{j+1}}{\Delta z}\right). \tag{21}$$

For consistency, the propagation velocity $c = z/\gamma$ also needs to be evaluated at the point $(k, j + 1/2)$. Therefore, we approximate the intermediate value of γ also by its mean, i.e.,

$$c_k^{j+1/2} = \left.\frac{z}{\gamma}\right|_k^{j+1/2} \approx \frac{z_k}{(\gamma_j + \gamma_{j+1})/2} = \frac{2z_k}{\gamma_j + \gamma_{j+1}}. \tag{22}$$

The resulting FD scheme is known to be stable (Strikwerda, 1989; Thomas, 1995). It is the simple tridiagonal implicit scheme given by

$$\underline{\boldsymbol{A}}\,\vec{p}^{\,j+1} = \underline{\boldsymbol{B}}\,\vec{p}^{\,j}, \tag{23}$$

where

$$\underline{\boldsymbol{A}} = \begin{pmatrix} 1 & \alpha_1 & 0 & & & \dots & 0 \\ -\alpha_2 & 1 & \alpha_2 & 0 & & \dots & 0 \\ 0 & -\alpha_3 & 1 & \alpha_3 & 0 & \dots & 0 \\ \vdots & & \ddots & \ddots & \ddots & \ddots & \vdots \\ 0 & \dots & 0 & -\alpha_{K-2} & 1 & \alpha_{K-2} & 0 \\ 0 & \dots & & 0 & -\alpha_{K-1} & 1 & \alpha_{K-1} \\ 0 & \dots & & & 0 & -\alpha_K & 1 \end{pmatrix} \tag{24}$$

and

$$\underline{\boldsymbol{B}} = \begin{pmatrix} 1 & -\alpha_1 & 0 & & & \dots & 0 \\ \alpha_2 & 1 & -\alpha_2 & 0 & & \dots & 0 \\ 0 & \alpha_3 & 1 & -\alpha_3 & 0 & \dots & 0 \\ \vdots & & \ddots & \ddots & \ddots & \ddots & \vdots \\ 0 & \dots & 0 & \alpha_{K-2} & 1 & -\alpha_{K-2} & 0 \\ 0 & \dots & & 0 & \alpha_{K-1} & 1 & -\alpha_{K-1} \\ 0 & \dots & & & 0 & \alpha_K & 1 \end{pmatrix}, \tag{25}$$

with

$$\alpha_k = -\frac{1}{2}\frac{z_k}{\gamma_j + \gamma_{j+1}}\frac{\Delta\gamma}{\Delta z} \qquad (k = 1, \dots, K). \tag{26}$$

This is a scheme that fulfills the requirement of being faster solvable than repeated migrations, since there are very fast methods for the inversion of tridiagonal matrices.

NUMERICAL EXAMPLE

We have implemented the above FD scheme and tested it for a simple synthetic data example in a homogeneous, elliptically anisotropic medium. The horizontal and vertical velocities are $u = 4500$ m/s and $v = 3000$ m/s, respectively. The model is depicted in Figure 1.

The synthetic data (see Figure 2) were generated by acoustic FD modeling where the medium ellipticity is simulated by an anisotropic density. For image-wave remigration, these synthetic data are the initial condition as a time-section can be understood as a time-migration with a migration velocity of $u = 0.0$ m/s.

As a first step, the synthetic data where propagated into the time-migrated domain under variation of the migration velocity using the FD image-wave remigration code of Novais et al. (2005). From the theory of Schleicher and Aleixo (2005, 2007), we know that the migration velocity for this propagation corresponds to the horizontal velocity of our elliptically anisotropic medium. This theory is confirmed from the resulting sequence of time-migrated images, some of which are depicted in Figures 3 to 8. At the migration velocities of $u = 3000$ m/s (Figure 3), $u = 3500$ m/s (Figure 4), and $u = 4000$ m/s (Figure 5), the bow-tie structure has not been fully resolved.

The image corresponding to a velocity value of $u = 4400$ m/s (Figure 6) is the first where the bow-tie structure is finally resolved. However, the same is true for velocities $u = 4500$ m/s (Figure 7) and $u = 4600$ m/s (Figure 8). Thus, from the images in Figures 6 to 8 alone, it is impossible to distinguish which of the corresponding velocity values is the correct one. Still, even from using only zero-offset data, we can estimate a velocity interval (here 4400 /ms to 4600 m/s) within which the correct migration velocity must lie. How diffractions can be used to improve this velocity estimate has been shown by Novais et al. (2005).

Of course, since our data are synthetic, we know the true velocity and the correct position of the time-migrated image. Figure 9 shows that actually, for the true horizontal velocity, the image is correctly positioned in time.

From this sequence of time-migrated images, we can draw the following conclusions:

- At the true vertical velocity, the image is out of focus.

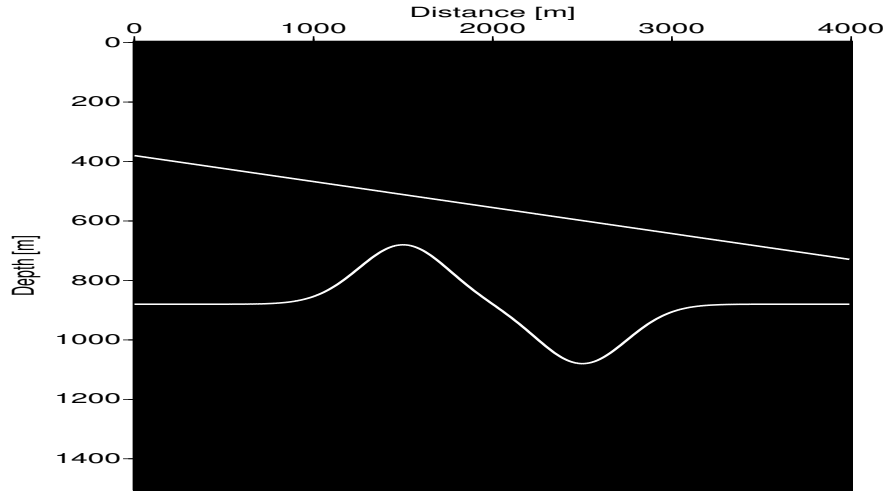

Figure 1: Model for the synthetic data experiment: Acoustic, elliptically anisotropic model, with horizontal and vertical velocities $u = 4500$ m/s and $v = 3000$ m/s, respectively.

- Both synclines and anticlines focus at the true horizontal velocity.
- Outside an interval around the true horizontal velocity, synclines or anticlines produce unresolved bow-tie structures.
- Therefore, a rough velocity estimate within an uncertainty interval is possible from zero-offset data using the imaging properties of curved reflectors.
- Using the horizontal velocity only, the time-migrated image is correctly positioned.
- Vertical velocities cannot be estimated from time processing of zero-offset data alone.

The last of the above observations remains true even if nonzero-offset data are used for the velocity analysis (Alkhalifah and Tsvankin, 1995). Therefore, the final time-migrated image of Figure 9 is the best we can hope for if our velocity analysis has worked perfect. For that reason, if our next step is a depth conversion using the time-migration velocity, we will end up with the wrong depth image depicted in Figure 10. Since the true vertical velocity is $v = 3000$ m/s, the depth of the reflectors is overestimated. Note that this does not just cause simple vertical shift of the reflector images. The dip of the upper reflector is represented wrongly, and so are the curvatures of the syncline and anticline structures. In accordance with the predicted depth stretch (equation 12), the overestimation of the reflector depth is the stronger the deeper the reflector is.

The isotropic depth-migrated image of Figure 10 has then been used as an initial condition for the image-wave propagation described by the vertical image-wave equation (equation 18). As for the propagation in horizontal velocity, the FD solution of this image-wave equation allows for the generation of a very dense sequence of migrated images corresponding to slightly varying values of γ. In this way, the originally isotropic depth-migrated image is becoming more and more anisotropic.

A subset of the so-obtained anisotropic images is depicted in Figures 11 to 15. We note that the image at $\gamma = 0.665$, which corresponds to a vertical velocity of $v = 3000$ m/s, images both reflectors at their true depth (see Figure 14). The distortion of reflector dips and curvatures is correctly removed. In Figure 15, which corresponds to $\gamma = 0.58$ or $v = 2610$ m/s, the depth stretch has already been overcorrected and the reflector images are too shallow.

From the sequence of images in Figures 11 to 15, we immediately recognize that a determination of the ellipticity or vertical velocity of the model from this kind of remigration only is impossible. Without

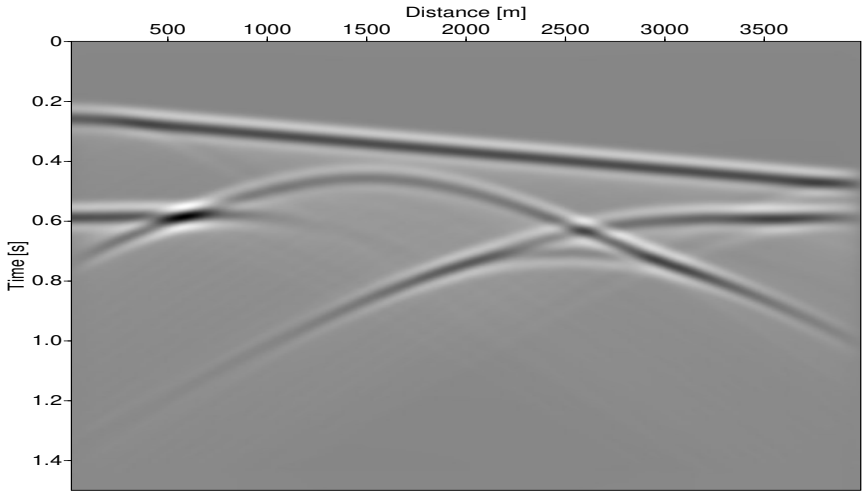

Figure 2: FD zero-offset data (correspond to a time migration with migration velocity $u = 0.0$ m/s):

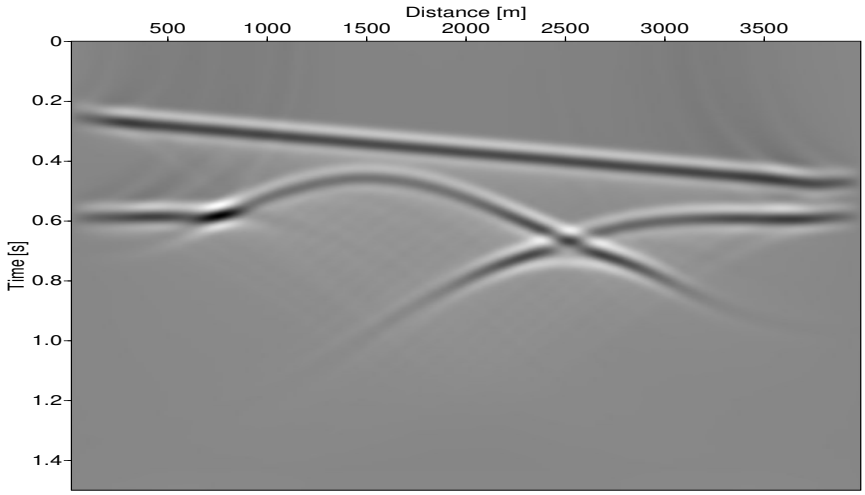

Figure 3: Image propagation to $u = 3000.0$ m/s.

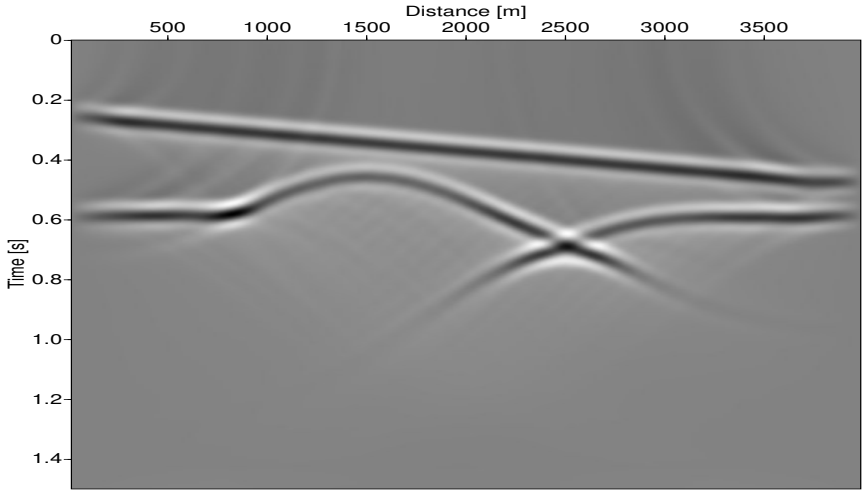

Figure 4: Image propagation to $u = 3500.0$ m/s.

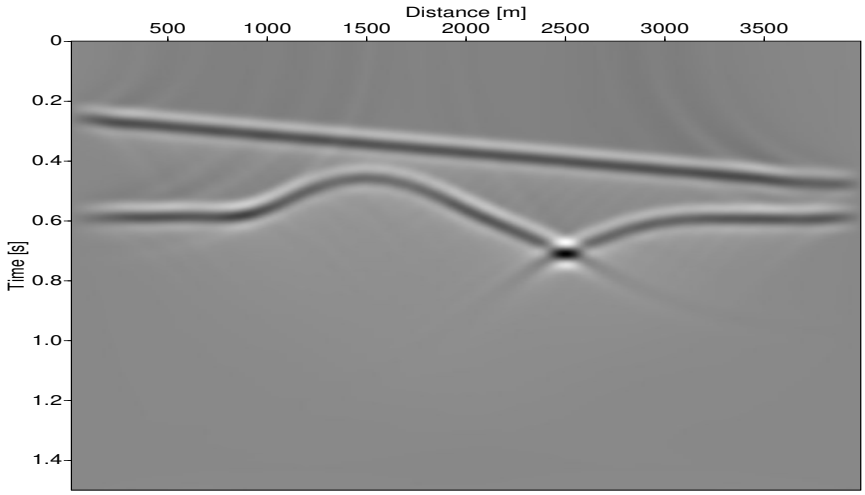

Figure 5: Image propagation to $u = 4000.0$ m/s.

the knowledge of the true reflector depth, there is no way of knowing which of these images is closest to the true geologic setting. However, with additional knowledge of the reflector depth at a single point, for instance at a well bore, a reasonable value of γ that ties the reflector to the well could be detected, thus resolving the positioning ambiguity.

SUMMARY & CONCLUSIONS

As observed by Fomel (1994) and Hubral et al. (1996), migrated reflector images for different migration velocities seem to "propagate" when the parameters of the migration velocity model are changed continuously. This effect can be described by partial differential equations, so-called "image wave equations." In homogeneous media, image-wave equations have been derived for various problems, describing the image propagation as a function of migration velocity and ellipticity. Extensions to inhomogeneous isotropic and anisotropic media have been attempted by Adler (2002) and Iversen (2002).

In this paper, we have derived the image-wave equation for depth remigration as a function of the unknown medium ellipticity, supposing that the horizontal velocity is known from time processing. In this situation, the dislocation of the reflector image is purely vertical.

The image-wave equation describing the problem of depth stretch due to the medium ellipticity is a simple one-dimensional one-way wave equation or advection equation with variable propagation velocity. As such, it is easy to find a stable FD implementation that simulates the image-wave propagation. The fact that this image-wave equation does not depend on the horizontal coordinates nor on the actual values of the horizontal and vertical velocities points towards its high potential of being useful in inhomogeneous media. Moreover, the equation remains the same for nonzero-offset data and can therefore even applied to the depth stretching of prestack migrated images.

A simple synthetic data example in a homogeneous, elliptically anisotropic model demonstrates that the present image-wave equation correctly positions reflector images in depth when the true medium ellipticity is reached. This can provide an easy means of well-tie improvement with simultaneous repositioning of the whole reflector image, together with providing an estimate of the medium ellipticity.

Of course, elliptic anisotropy is a rather simplistic approximation to the real world. Nonetheless, it can be considered an ideal link from isotropy to anisotropy. Compared to isotropy, it presents an additional degree of freedom that should be sufficient in many cases to improve well-ties by simple ellipticity propagation of the migrated image, On the other hand, compared to more realistic types of anisotropy, it has the advantage that only one additional parameter needs to be determined from the data. Thus, elliptical anisotropy should be thought of as a lowest-order approximation to more realistic situations.

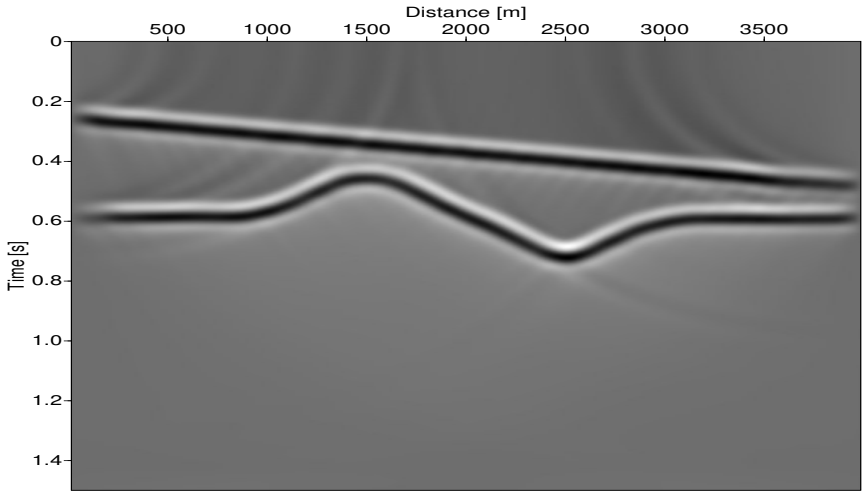

Figure 6: Image propagation to $u = 4400.0$ m/s.

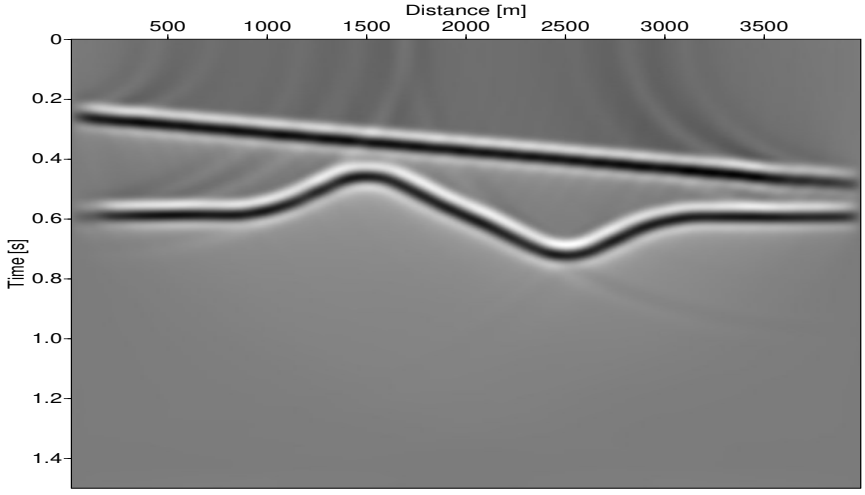

Figure 7: Image propagation to $u = 4500.0$ m/s.

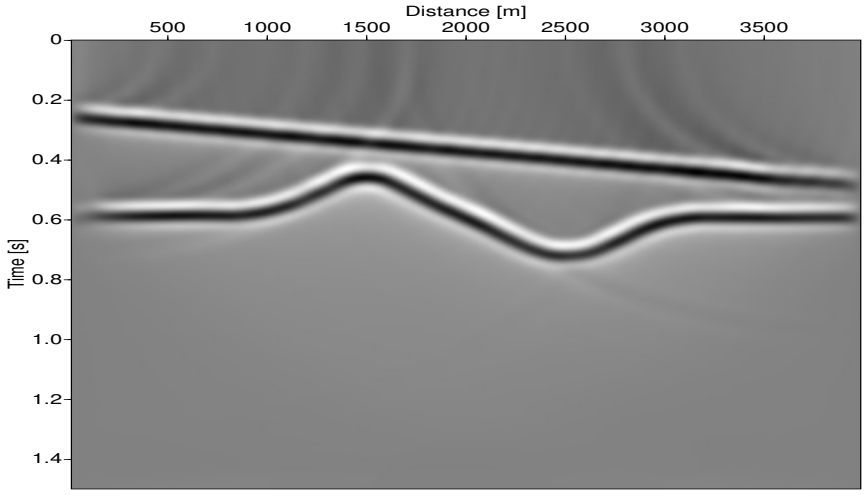

Figure 8: Image propagation to $u = 4600.0$ m/s.

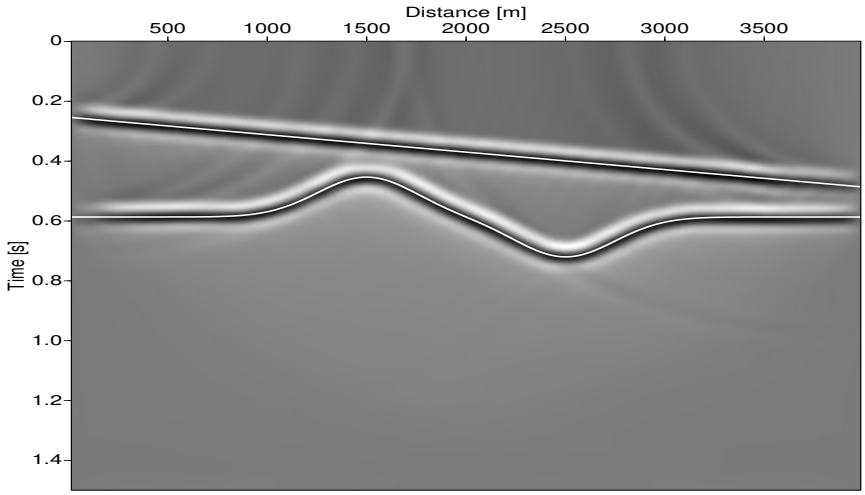

Figure 9: Image propagation to $u = 4500.0$ m/s. Also shown as white lines are the correct positions of the reflector images in a time-migrated section.

ACKNOWLEDGMENTS

We thank the Brazilian research agencies, CAPES, CNPq and FAPESP, and the sponsors of the Wave Inversion Technology (WIT) consortium for their support.

REFERENCES

Adler, F. (2002). Kirchhoff image propagation. *Geophysics*, 67(1):126–134.

Aleixo, R. and Schleicher, J. (2004). Image-wave remigration in elliptically anisotropic media. *Annual WIT Report*, 8:131–139.

Alkhalifah, T. and Tsvankin, I. (1995). Velocity analysis for transversely isotropic media. *Geophysics*, 60(05):1550–1566.

Fomel, S. (1994). Method of velocity continuation in the problem of seismic time migration. *Russian Geology and Geophysics*, 35(5):100–111.

Fomel, S. (2003a). Time migration velocity analysis by velocity continuation. *Geophysics*, 68(5):1662–1672.

Fomel, S. (2003b). Velocity continuation and the anatomy of residual prestack time migration. *Geophysics*, 68(5):1650–1661.

Hubral, P., Tygel, M., and Schleicher, J. (1996). Seismic image waves. *Geophysical Journal International*, 125(2):431–442.

Iversen, E. (2002). From approximate to accurate velocity rays. In *64th Ann. Internat. Mtg., EAGE*, pages P107:1–4. EAEG.

Jaya, M. (1997). *Imaging reflection seismic data using the method of velocity continuation*. Dissertation, Universität Karlsruhe (TH).

Jaya, M. S., Botelho, M., Hubral, P., and Liebhardt, G. (1999). Remigration of ground-penetrating radar data. *Journal of Applied Geophysics*, 41:19–30.

Larner, K. and Beasley, C. (1987). Cascaded migration: Improving the accuracy of finite-difference migration. *Geophysics*, 52(5):618–643.

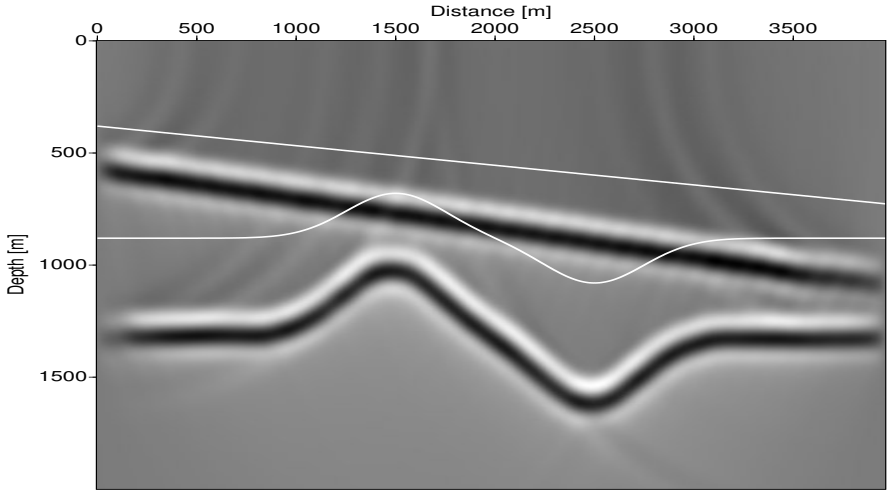

Figure 10: Depth conversion of the final time migrated image of Figure 7 using the best possible time-migration velocity $v = 4500.0$ m/s. Also shown as white lines are the true positions of the reflectors.

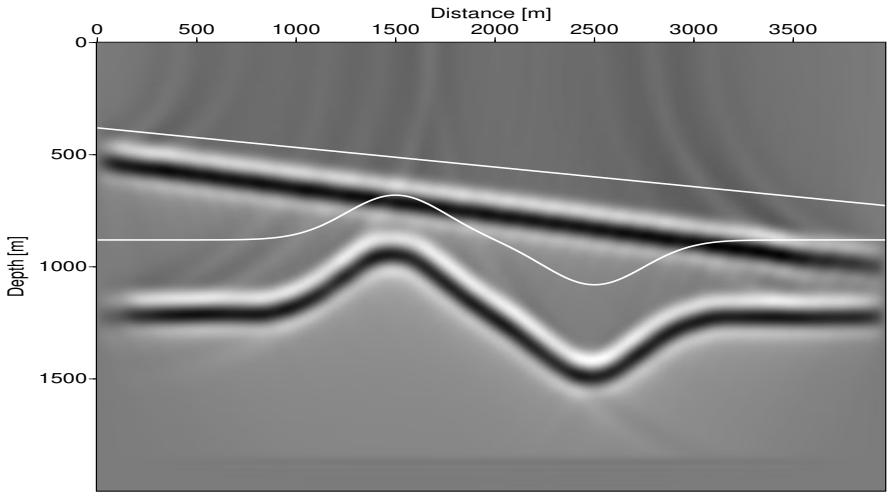

Figure 11: Image propagation to $\gamma = 0.92$, i.e., $v = 4140.0$ m/s

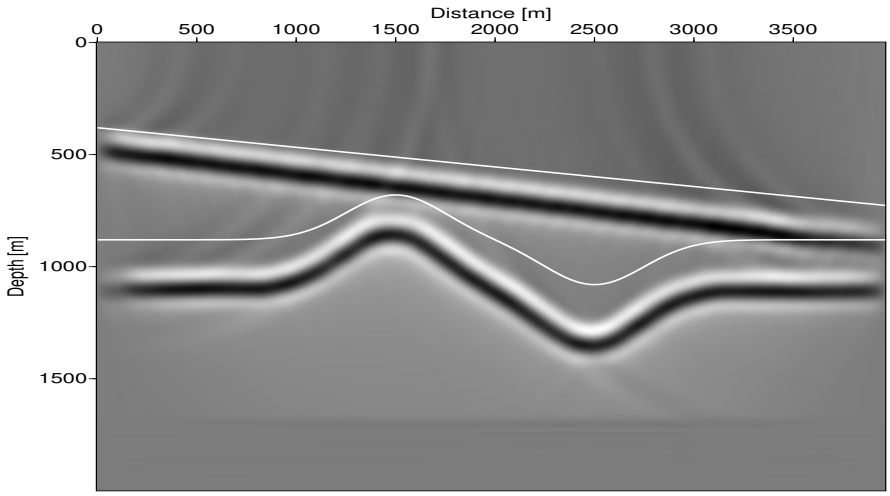

Figure 12: Image propagation to $\gamma = 0.835$, i.e., $v = 3760.0$ m/s

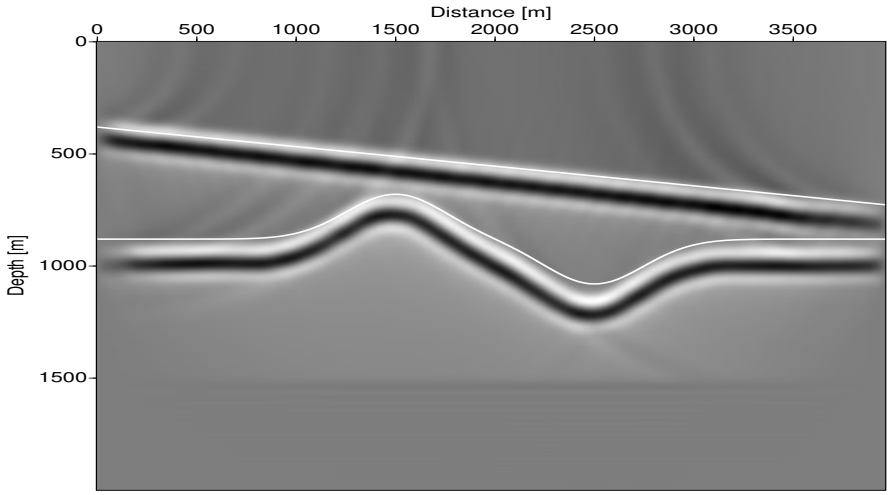

Figure 13: Image propagation to $\gamma = 0.75$, i.e., $v = 3380.0$ m/s

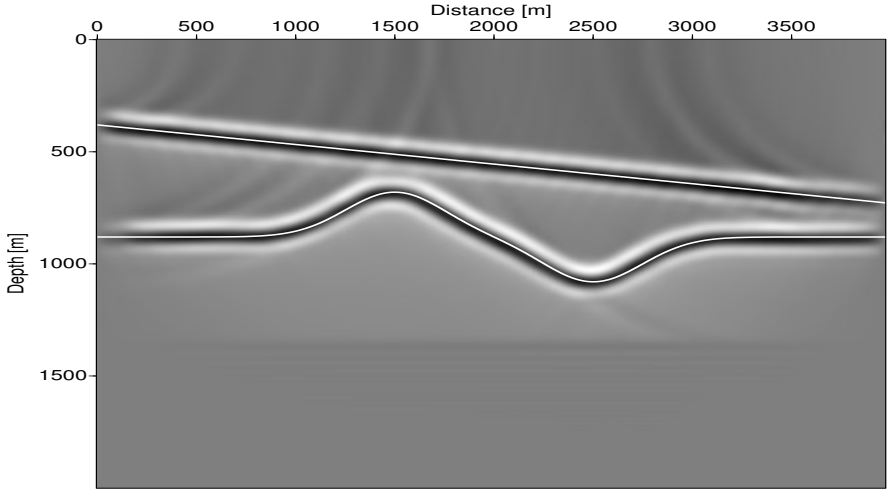

Figure 14: Image propagation to $\gamma = 0.665$, i.e., $v = 3000.0$ m/s

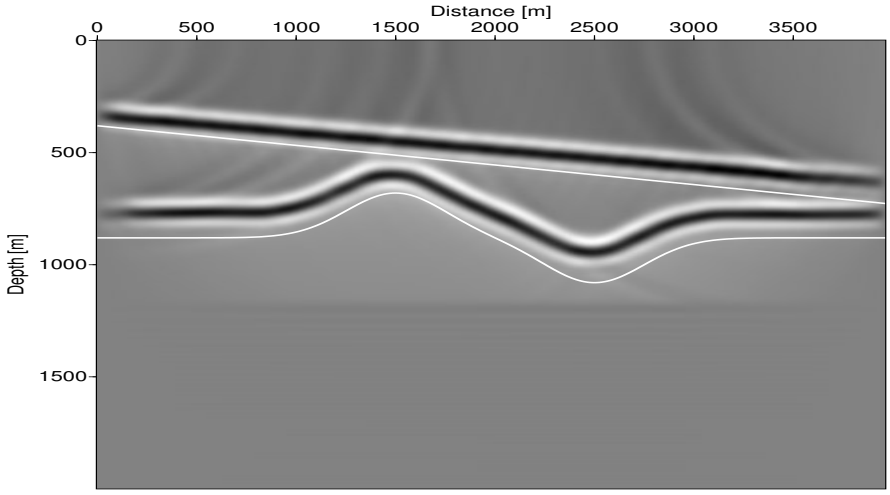

Figure 15: Image propagation to $\gamma = 0.58$, i.e., $v = 2610.0$ m/s

Novais, A., Costa, J., and Schleicher, J. (2005). Velocity determination by image-wave remigration. *Annual WIT Report*, 9:66–75.

Rocca, F. and Salvador, L. (1982). Residual migration. In *52nd Ann. Internat. Mtg., SEG*, Dallas. SEG.

Rothman, D., Levin, S., and Rocca, F. (1985). Residual migration: Applications and limitations. *Geophysics*, 50(1):110–126.

Schleicher, J. and Aleixo, R. (2005). Time and depth remigration in elliptically anisotropic media using image-wave propagation. *Annual WIT Report*, 9:76–87.

Schleicher, J. and Aleixo, R. (2007). Time and depth remigration in elliptically anisotropic media using image-wave propagation. *Geophysics*. in print.

Schleicher, J., Novais, A., and Munerato, F. P. (2004). Migration velocity analysis by depth image-wave remigration: First results. *Geophysical Prospecting*, 52:559–573.

Strikwerda, J. C. (1989). *Finite Difference Schemes and Partial Differential Equations*. Wadsworth & Brooks, California.

Thomas, J. W. (1995). *Numerical Partial Differential Equations*. Springer-Verlag, New York.

APPENDIX A

DERIVATION FOR OFFSET DATA

For a source-receiver pair displaced along the x axis with half-offset h from one another, the reflection traveltime (equation 4) reads

$$T(\xi,\eta;x,y,z) = \frac{1}{u}(S+R), \tag{27}$$

where

$$S = \sqrt{[x-(\xi-h)]^2+(y-\eta)^2+\gamma^2 z^2}, \tag{28}$$

$$R = \sqrt{[x-(\xi+h)]^2+(y-\eta)^2+\gamma^2 z^2}. \tag{29}$$

As before, this traveltime must not vary when changing γ to γ_0, i.e., $T(\xi,\eta;x,y,z)$ must be equal to

$$T(\xi,\eta;x_0,y_0,z_0) = \frac{1}{u}(S_0+R_0), \tag{30}$$

where

$$S_0 = \sqrt{[x_0-(\xi-h)]^2+(y_0-\eta)^2+\gamma_0^2 z_0^2}, \tag{31}$$

$$R_0 = \sqrt{[x_0-(\xi+h)]^2+(y_0-\eta)^2+\gamma_0^2 z_0^2}. \tag{32}$$

Thus, the offset version of equation 6 reads

$$F = S+R-S_0-R_0 = 0. \tag{33}$$

The condition that the derivatives of F with respect to ξ and η must be zero yields

$$\frac{\xi-h-x}{S}+\frac{\xi+h-x}{R} = \frac{\xi-h-x_0}{S_0}+\frac{\xi+h-x_0}{R_0} \tag{34}$$

$$\frac{\eta-y}{S}+\frac{\eta-y}{R} = \frac{\eta-y_0}{S_0}+\frac{\eta-y_0}{R_0}. \tag{35}$$

It is clear that the last three equations are simultaneously fulfilled by the relationships between the coordinates given in equations 9, 10, and 12. Consequently, the remaining considerations remain the same as discussed in the zero-offset case.

Alternative derivation

Another way of expressing the independence of the traveltime (equation 27) of γ is by requiring γ to depend in such a way on the coordinates (x, y, z) of the reflection point that a change in these coordinates does not imply a change in traveltime. In other words, after substituting the image-wave eikonal $\gamma = \Gamma(x, y, z)$ in the reflection traveltime (equation 27), we must require that the total derivative of $T(\xi, \eta; x, y, z)$ with respect to the coordinates be zero, i.e.,

$$\frac{dT}{dx} = 0 \quad = \quad \frac{\partial T}{\partial x} + \frac{\partial T}{\partial \gamma}\frac{\partial \Gamma}{\partial x}, \tag{36}$$

$$\frac{dT}{dy} = 0 \quad = \quad \frac{\partial T}{\partial y} + \frac{\partial T}{\partial \gamma}\frac{\partial \Gamma}{\partial y}, \tag{37}$$

$$\frac{dT}{dz} = 0 \quad = \quad \frac{\partial T}{\partial z} + \frac{\partial T}{\partial \gamma}\frac{\partial \Gamma}{\partial z}. \tag{38}$$

From these identities, we immediately obtain the following expressions for the derivatives of the image-wave eikonal $\Gamma(x, y, z)$

$$\frac{\partial \Gamma}{\partial x} \quad = \quad -\frac{\partial T}{\partial x} \Big/ \frac{\partial T}{\partial \gamma}, \tag{39}$$

$$\frac{\partial \Gamma}{\partial y} \quad = \quad -\frac{\partial T}{\partial y} \Big/ \frac{\partial T}{\partial \gamma}, \tag{40}$$

$$\frac{\partial \Gamma}{\partial z} \quad = \quad -\frac{\partial T}{\partial z} \Big/ \frac{\partial T}{\partial \gamma}. \tag{41}$$

The partial derivatives of $T(\xi, \eta; x, y, z)$ with respect to γ and the coordinates x, y, and z are easily calculated as

$$\frac{\partial T}{\partial \gamma} \quad = \quad \frac{1}{u\,S}\Gamma z^2 + \frac{1}{u\,R}\Gamma z^2 = \frac{1}{u}\Gamma z^2\left(\frac{1}{S} + \frac{1}{R}\right), \tag{42}$$

$$\frac{\partial T}{\partial x} \quad = \quad \frac{x - \xi + h}{u\,S} + \frac{x - \xi - h}{u\,R}, \tag{43}$$

$$\frac{\partial T}{\partial y} \quad = \quad \frac{1}{u\,S}(y - \eta) + \frac{1}{u\,R}(y - \eta) = \frac{y - \eta}{u}\left(\frac{1}{S} + \frac{1}{R}\right), \tag{44}$$

$$\frac{\partial T}{\partial z} \quad = \quad \frac{1}{u\,S}\Gamma^2 z + \frac{1}{u\,R}\Gamma^2 z = \frac{1}{u}\Gamma^2 z\left(\frac{1}{S} + \frac{1}{R}\right). \tag{45}$$

We now need to use these equations to eliminate ξ and η from equations 39 to 41. Though equations 42 to 45 are high-order equations in ξ and η that are hard to solve, this elimination can easily be achieved by substitution of equations 42 and 45 in expression 41. This yields

$$\frac{\partial \Gamma}{\partial z} = -\frac{\Gamma}{z}, \tag{46}$$

which is identical to the zero-offset image-wave eikonal equation (equation 16). Therefore, the image-wave equation for the nonzero-offset case is again given by

$$p_z = \frac{\gamma}{z} p_\gamma. \tag{47}$$